

1 **Internal structure and significance of ice-marginal moraine in the Kebnekaise**
2 **Mountains, northern Sweden**

3 Tonkin, T. N., Midgley, N. G., Graham, D. J. & Labadz, J. C.: Internal structure and
4 significance of ice-marginal moraine in the Kebnekaise Mountains, northern Sweden.
5 *Boreas*. 10.1111/bor.12220. ISSN 0300-9483.

6 **Abstract**

7 Despite a long history of glaciological research, the palaeo-environmental significance
8 of moraine systems in the Kebnekaise Mountains, Sweden, has remained uncertain.
9 These landforms offer the potential to elucidate glacier response prior to the period of
10 direct monitoring and provide an insight into the ice-marginal processes operating at
11 polythermal valley glaciers. This study set out to test existing interpretations of
12 Scandinavian ice-marginal moraines, which invoke ice stagnation, pushing,
13 stacking/dumping and push-deformation as important moraine forming processes.
14 Moraines at Isfallsglaciären were investigated using ground-penetrating radar to
15 document the internal structural characteristics of the landform assemblage. Radar
16 surveys revealed a range of substrate composition and reflectors, indicating a debris-
17 ice interface and bounding surfaces within the moraine. The moraine is demonstrated
18 to contain both ice-rich and debris-rich zones, reflecting a complex depositional history
19 and a polygenetic origin. As a consequence of glacier overriding, the morphology of
20 these landforms provides a misleading indicator of glacial history. Traditional
21 geochronological methods are unlikely to be effective on this type of land- form as the
22 fresh surface may post-date the formation of the landform following reoccupation of
23 the moraine rampart by the glacier. This research highlights that the interpretation of
24 geochronological data sets from similar moraine systems should be undertaken with
25 caution.

26 *Toby N. Tonkin (t.tonkin@derby.ac.uk), Department of Natural Sciences, University of*
27 *Derby, Kedleston Road, Derby, DE22 1GB, UK; Nicholas G. Midgley and Jillian C.*
28 *Labadz, School of Animal, Rural and Environmental Sciences, Nottingham Trent*
29 *University, Brackenhurst Campus, Southwell, Nottinghamshire, NG25 0QF, UK; David*
30 *J. Graham, Polar and Alpine Research Centre, Department of Geography,*
31 *Loughborough University, Leicestershire, LE11 3TU, UK; received 8th July 2016,*
32 *accepted 3rd November 2016.*

33 **Introduction**

34 The moraines developed across Scandinavia have a long history of geomorphological
35 research (e.g. Schytt 1959; Karlén 1973; Shakesby et al. 1987; Matthews et al. 1995;
36 Etienne et al. 2003; Hayman & Hättestrand 2006; Winkler & Matthews 2010;
37 Matthews et al. 2014), and have served as early study sites for ice-cored landforms
38 (Østrem 1959, 1963, 1964, 1965; Ackert 1984). Specifically, Østrem (1964)
39 recognised that some moraines in Scandinavia are disproportionately large in size
40 compared to the glaciers that formed them, suggesting the presence of buried ice. The
41 formation of such moraine complexes has been subject to uncertainty surrounding: (i)
42 the origin of ice (Schytt 1959; Østrem 1963, 1964; Ackert 1984); (ii) the distinction
43 between ice-marginal moraine complexes and rock glaciers (Barsch 1971; Østrem
44 1971); and (iii) the interaction between existing moraine ramparts and advancing
45 glaciers in permafrost terrain (Matthews & Shakesby 1984; Shakesby et al. 1987,
46 2004; Matthews et al. 2014). Ice-cored moraines are commonly found at the margins
47 of terrestrially terminating glaciers (Krüger & Kjær 2000; Schomacker & Kjær 2008;
48 Midgley et al. 2013; Tonkin et al. 2016); however, the long-term preservation of ice is
49 typically limited under an ameliorating climate. In areas characterized by permafrost,
50 ice-cored terrain can be preserved over longer time scales (Sugden et al. 1995). A
51 typical ice-cored moraine is composed of relict glacier ice that becomes isolated from
52 the glacier terminus under a sufficiently thick debris cover (Goldthwait 1951; Østrem
53 1959, 1964; Evans 2009). Whilst researchers have observed glacier ice within the
54 structure of ice-marginal moraines in Scandinavia (Schytt 1959; Ackert 1984), after
55 analysing the crystallographic properties, Østrem (1963) highlighted that ice within
56 moraines could be of meteoric origin, and may originate as a moraine distal snowbank
57 that was subsequently overridden by an advancing glacier and incorporated into the
58 internal structure of ice-marginal landforms (Østrem 1963, 1964). However, Østrem
59 (1964) also acknowledged that buried ice may have a complex origin, with the potential
60 for stagnating glacier ice to also be incorporated into moraine structure (e.g. 'controlled
61 moraine'; see Evans 2009), but considered that to some extent, most large moraines
62 contained varying quantities of snowbank ice. In recent years, the term 'Østrem' type
63 moraine has been introduced in the literature (e.g. Whalley 2009) to distinguish these
64 moraine systems from ice-cored moraine counterparts in the high-Arctic that
65 predominantly contain glacier ice (Evans 2009). Ice-cored moraines have also been

66 interpreted as rock glaciers (e.g. Barsch 1971). Whilst a polygenetic interpretation
67 could be appropriate for some ice-cored moraines that may transition into rock glaciers
68 (Whalley & Martin 1992; Berthling 2011), geomorphologically stable features
69 deposited on near-level terrain were cited by Østrem (1971) as suitable criteria for
70 classifying features as ice-cored moraine.

71 Karlen (1973) argued for 'proximal enlargement' as an important moraine forming
72 process in northern Sweden. Karlen envisaged a scenario where moraine ramparts
73 acted as a topographic barrier for subsequent glacier advances, leading to the
74 incremental stacking of imbricate 'drift sheets' onto ice-proximal slopes. These 'drift
75 sheets' were proposed to correspond to successive episodes of Holocene glacier
76 expansion. This hypothesis was favoured despite ground-level photographical
77 evidence from c. 1910 depicting various glaciers in northern Sweden partially
78 overriding their respective moraine complexes (Karlen 1973).

79 Conversely, in southern Norway a 'push deformation' hypothesis has been proposed
80 in which post depositional modification of existing moraine results from a subsequent
81 glacier advance. The transmission of stress is suggested to result in moraine
82 complexes with a series of anastomosing ridges, and steep proximal and distal slope
83 angles (Shakesby et al. 1987). This hypothesis, which differs from Østrem (1964) who
84 considered the overriding and distal deposition of ridges as an important moraine
85 forming process, has been demonstrated to be important in the Breheimen and
86 Jotunheimen regions of southern Norway (Matthews et al. 2014). However, Matthews
87 et al. (2014) highlighted that additional geophysical survey work is required to validate
88 the exact mechanisms of moraine formation and modification.

89 The glaciers of the Kebnekaise region have been subject to significant glaciological
90 research (e.g. Schytt 1962, 1966; Holmlund et al. 1996; Holmlund & Jansson 1999;
91 Zemp et al. 2010; Rippin et al. 2011; Gusmeroli et al. 2012; Brugger & Pankratz 2015).
92 However, despite considerable research also investigating moraine development (e.g.
93 Østrem 1964; Karlen 1973; Etienne et al. 2003; Heyman & H€attestrand 2006), the
94 full palaeo-environmental and glaciological significance of the landforms remains
95 unclear. This is at odds with the importance of these sites for contextualizing current
96 and future glacier change. The potential snowbank origin of ice contained within these
97 moraines, the various competing hypotheses in relation to their mode of formation and

98 the potential post depositional modification of these landforms distinguishes them from
99 other ice-cored moraine, yet there is a paucity of research that investigates the
100 significance of these geomorphological features. A modern investigation of the
101 characteristics of these features is therefore warranted.

102 This study set out to test existing interpretations of Scandinavian ice-marginal
103 moraines, which invoke ice stagnation, pushing, stacking/dumping and deformation as
104 important moraine forming processes. The objectives of this research were therefore
105 to: (i) document the structural character of moraines at Isfallsglaciären using ground-
106 penetrating radar (GPR); (ii) infer the mode of formation and palaeoglaciological
107 significance of the moraine complex developed at Isfallsglaciären; and (iii) examine
108 the wider implications in relation to the use of Scandinavian moraines as a palaeo-
109 environmental proxy. This work is important because Isfallsglaciären has been
110 dynamic over the course of the Holocene and the moraines provide insight into these
111 changes prior to the period of direct measurements and observations.

112 *Overview of study site*

113 Isfallsglaciären is a ~1.5-km long valley glacier located in the Kebnekaise Mountains
114 in northern Sweden (Fig. 1). The glacier has an easterly aspect and has receded ~500
115 m from the recent maximum extent in the 1920s, when the glacier overrode the inner
116 moraine ridge (e.g. Østrem 1963; Karlén 1973). Like the neighbouring Storglaciären,
117 Isfallsglaciären is polythermal in character (Eklund & Hart 1996). Schytt (1962), for
118 example, recorded subfreezing temperatures in an artificially created tunnel at the
119 glacier terminus. Storglaciären is currently undergoing changes to its thermal
120 configuration (Pettersson et al. 2003), with one third of its cold surface layer lost over
121 the 1989– 2009 period (Gusmeroli et al. 2012). These changes have been linked to
122 recent climatic amelioration, such as increased winter air temperatures since the
123 1980s (Pettersson et al. 2003; Gusmeroli et al. 2012). It is likely that the thermal regime
124 of Isfallsglaciären is undergoing a similar evolution.

125 The morphology of the Isfallsglaciären moraines has previously been described by
126 Schytt (1959) and Karlén (1973). In this study, the moraine complex is split into three
127 zones based on morphological criteria (Fig. 1). Within the outer-frontal zone (Z_i), a
128 subdued moraine ridge attains a relief of ~10 m above the surrounding terrain. A series
129 of discontinuous mounds are present on the distal slope of this ridge. Within the inner-

130 frontal zone (Zii), a moraine ridge rises up to ~20 m above the surrounding terrain.
131 Moraines in Zii are over-printed with flutes related to overriding of the ridge by a glacier
132 advance in 1910 (Karlen 1973). Within the lateral complex (Ziii), a lateral moraine of
133 significant topographical prominence rises ~20–30 m above the surrounding terrain.
134 This feature displays a furrowed morphology and includes a prominent arcuate ridge.
135 A semi-permanent snowbank occurs on the distal slope of this feature (e.g. Østrem
136 1964; Karlen 1973).

137 *Materials and methods*

138 Radar data were collected using a Pulse EKKO Pro GPR in spring 2013 under winter
139 conditions to ensure frozen ground. Reflection surveys were undertaken with a 100
140 MHz perpendicular broadside antenna configuration using a 0.25-m step size between
141 traces and a 1-m transmitter/receiver separation distance. A distance of >5 m
142 was kept between the control unit and transmitter/receiver setup to minimize signal
143 interference. Traces were manually triggered using either the control unit interface or
144 a CANBUS electrical beeper and used a time window of 800 ns. Surveys were
145 conducted along a 100-m tape to ensure that the correct step-size was maintained
146 throughout the survey. To correct radar profiles for topography, height was surveyed
147 on each transect using an automatic level. A Garmin GPSMap 62 was also used to
148 record the start and finish location of each transect. During common mid-point/wide-
149 angle reflection-refraction (CMP/ WARR) surveys, the fibre optic cables (each of which
150 were 20 m in length) limited the maximum separation to 38 m, with WARR surveys
151 using a common receiver configuration. Post-processing of CMP/WARR and reflection
152 data was conducted using the EKKO_View Deluxe software from Sensors and
153 Software. Three post-processes were applied to reflection profiles: (i) dewow; (ii)
154 topographical correction; and (iii) gain control. Automatic gain control (AGC) was
155 applied to six of the seven survey profiles. For a single profile, constant gain was found
156 to provide a clearer visualization of subsurface features, so it was used in place of
157 AGC.

158 The radar data were interpreted qualitatively following post-processing. Terminology
159 used to describe radar facies and surfaces was adopted from Neal (2004), Pellicer &
160 Gibson (2011) and Lindhorst & Schutter (2014). Four main characteristics for reflectors
161 were noted: (i) the reflector shape (planar, wavy, convex, concave); (ii) the reflector

162 dip (horizontal, or either up- or down-glacier dipping); (iii) the relationship between
163 different reflectors within a radargram (parallel, subparallel, oblique, chaotic); and (iv)
164 the continuity of reflectors within a radargram (continuous, moderately continuous or
165 discontinuous). Sedimentology was assessed under summer conditions via shallow
166 excavations (<1 m) to 'ground truth' the observed radar-facies. Facies were assessed
167 using the Hambrey (1994) classification for poorly sorted sediments. Clasts (samples
168 of $n = 50$ per facies) were assessed for shape and roundness (Powers 1953; Benn
169 2004); however, it was not feasible to record clast shape for boulder-gravel facies.
170 Shape (C40) and roundness (RA) indices were calculated to facilitate discrimination
171 between samples (e.g. Benn & Ballantyne 1994). These data are presented alongside
172 the reflection data sets.

173 **Results**

174 *Radar propagation velocity*

175 WARR and CMP data sets were processed to obtain radar-wave velocities (Fig. 2).
176 Two surveys were completed per zone (Zi, Zii and Ziii; Fig. 1). Outer-frontal (Zi)
177 surveys (A and B) and inner-frontal (Zii) surveys (C and D) all provided similar radar
178 velocities at ~ 0.11 m ns⁻¹. The velocities were located at a two-way travel time of <150
179 ns, indicating strong signal attenuation. The lateral complex (Ziii) was broadly found
180 to exhibit higher propagation velocities. Specifically, values of ~ 0.15 m ns⁻¹ are
181 identified on both lateral complex surveys (E and F). These are detected at a time
182 window of 100–300 ns.

183 *Reflection surveys and surficial sedimentology*

184 *Outer-frontal (Zi).* – Profiles 1 and 2 both ran transverse to the ridge crestline in the
185 outer-frontal zone (Zi) (distal slope to the right; Fig. 3; Table 1). Profile 1 appeared to
186 be more structurally diverse, with the proximal slope of the landform intersected by a
187 clear up-glacier dipping reflector. Ground truth surveys under summer conditions
188 found a topographically prominent facies of mud on the proximal slope, which related
189 to this radar surface. Below this feature a series of discontinuous, up-glacier dipping
190 reflectors were also visible. Reflectors within the crest of the landform were irregular
191 and hyperbolic, and corresponded to deposits of diamicton (% RA = 52; C40 = 16). On
192 the distal slope of this landform, coherent, continuous reflectors were visible within a
193 topographically prominent hummock (profile 1). Summer surveys found gravel (% RA

194 = 40; C40 = 10) interspersed with stratified granular and sandy beds. With the
195 application of AGC, structure was poorly defined at depth within the main ridge.

196 Profile 2 displayed multiple overlapping hyperbolic point diffractions and irregular
197 medium and high amplitude reflectors. Unlike profile 1, a partially coherent down-
198 glacier dipping reflector appeared to dissect the feature between ~27 and 35 m and
199 also corresponded with a change in surface morphology. Excavations revealed that
200 diamicton was present both above and below this reflector. The upper diamicton facies
201 was found to contain a higher percentage of angular clasts (% RA = 76; C40 = 28
202 and % RA = 72; % C40 = 16) than the lower unit (% RA = 62; C40 = 14 and % RA
203 = 60; C40 = 12). Up-glacier dipping reflectors were also present at depth within the
204 landform and could be seen ~20–30 and ~40–50 m along the profile.

205 *Inner-frontal (Zii).* – The inner-frontal ridge was surveyed in profile 3. Shallow
206 excavations (<1 m) along this feature uncovered diamicton with a subangular clast
207 component (% RA = 54; % C40 = 12). The crestline of profile 3 was overprinted with
208 subglacial flutes. The main features of structural interest within this profile were
209 coherent, high amplitude reflectors, which were visible between ~67 and 96 m. The
210 reflectors initially ran subparallel with the moraine surface, before dipping down-
211 glacier. A second less coherent reflector was present at 88–96 m.

212 *Lateral complex (Ziii).* – Profile 4 covered the area where the frontal and lateral
213 moraine sections of the landform adjoined. Atypical of other reflection surveys,
214 continuous reflectors could be seen running sub-parallel to the moraine surface. At
215 ~28 m along this transect two coherent reflectors could be seen to cross-cut each
216 other. A radar facies characterized by irregular reflectors and overlapping hyperbolic
217 point diffractions was seen both above and below these coherent reflectors. The ridge
218 crest was found to contain a facies of diamicton with a subangular component (% RA
219 = 46; % C40 = 32).

220 Profiles 5, 6 and 7 displayed the subsurface structure of the southern-lateral complex.
221 Profile 5 ran oblique to the landform (but approximately parallel to the inferred direction
222 of former ice flow). The sedimentology along profiles 5–7 was predominantly angular
223 boulder-gravel with the exception of the small ridge captured in profile 5, which
224 contained diamicton (% RA = 62; C40 = 14) and gravel (% RA = 66; C40 = 16) with
225 down-glacier dipping granular lenses. Similar to other profiles, profile 5 displayed

226 hyperbolic (related to subsurface point diffractions) and irregular reflectors. Two
227 coherent sub-surface reflectors initially ran approximately parallel to the moraine
228 surface, but subsequently dipped down-glacier. These were visible between ~0–14
229 and 25–47 m along profile 5, respectively.

230 Profile 6 ran transverse to the southern lateral moraine complex. Here, the main
231 structural feature was a moderately continuous reflector at depth within the moraine.
232 This reflector appeared to run subparallel to the moraine surface and was both over-
233 and underlain by hyperbolic, chaotic and irregular radar facies. A rounded response
234 occurred mid profile (~45–55 m). A snowbank could be distinguished on the ice-distal
235 slope of the landform. The base of the ice-distal slope was characterized by multiple
236 strong point diffractions. Profile 7 ran approximately parallel to the ridge crest of the
237 southern-lateral complex. The main structural feature of interest within this profile
238 could be seen between ~50 and ~130 m along the profile and was located in the ~50
239 to 70 ns time window. This feature ran subparallel to the moraine surface and
240 appeared to dissect an upper radar-facies consisting of hyperbolic and irregular point
241 diffractions. A less coherent (partially due to the hyperbolic nature of the shallower
242 radar-facies) continuation of this radar surface was present 0 to 20 m along profile 7
243 at ~45 ns. The near-surface sedimentology along profiles 6 and 7 was predominantly
244 boulder-gravel and diamicton. The percentage of subangular clasts within the boulder-
245 gravel surface facies across Zii increased progressively down-moraine (% RA = 96,
246 98, 88, 66 and 48). Diamicton sampled from facies in proximity to profiles 6 and 7 had
247 a predominantly angular clast component (% RA = 74; C40 = 20 and 74; C40 = 26).

248 **Interpretation**

249 *Radar wave velocities and likely composition*

250 The propagation velocity of radar waves is related to the subsurface composition (Neal
251 2004). Thus, by relating the velocities obtained to values for known substrates (Table
252 2), the sedimentological characteristics of the landforms can be inferred. Radar-wave
253 propagation velocity also varies depending on the saturation and thermal state (e.g.
254 frozen or unfrozen) of a material (Neal 2004). Here, moraine composition appears to
255 vary spatially across the lateral-frontal complex. The surveys undertaken in the inner-
256 frontal (Zii) and outer-frontal (Zi) zones indicate that these areas are debris-rich.
257 Schwamborn et al. (2008) found frozen diamicton (with 10% pore water) to have a

258 radar-wave velocity of 0.125 m ns^{-1} (determined from a CMP survey). This contrasts
259 with unfrozen diamictons and till, which exhibit propagation velocities of $0.06\text{--}0.09 \text{ m}$
260 ns^{-1} (e.g. Burki et al. 2009; Lukas & Sass 2011). Given that the moraines were frozen
261 at the time of the survey, slightly higher velocities are to be expected, especially if
262 sediment is partially saturated prior to winter freezing. Velocities recorded from the
263 inner-frontal (Zii) and outer-frontal (Zi) zones (surveys A–D; $\sim 0.11 \text{ m ns}^{-1}$) are,
264 therefore, consistent with a composition of diamicton with a limited volume of
265 interstitial ice; a finding also consistent with surveys of surface sedimentology (Table
266 1). It is unclear whether the strong signal attenuation resulting from the thick silt-rich
267 diamicton facies (hence shallow coherent reflections visible in the velocity-depth plots)
268 is masking ice-rich permafrost at depth within the topographically prominent inner-
269 frontal moraine (Zii).

270 The structural composition of the lateral complex (Ziii) is less straightforward, but is
271 highly likely to indicate the presence of ice within the landform. Here, the wide range
272 of radar propagation velocities (Fig. 2) most likely results from variability in the porosity,
273 amount of interstitial ice and fine material within the landform. Østrem (1963, 1964)
274 directly observed ice within the southern lateral moraine by excavating a series of pits.
275 More recently, Kneisel (2010) detected ice-rich permafrost in moraine at
276 Isfallsglaciären using electrical resistivity tomography (ERT) with surveys undertaken
277 where the lateral and frontal moraines adjoin (C Kneisel, pers. comm. 2013). Given
278 the coarse nature of the surficial sediments (boulder-gravel facies) and known
279 inclusion of ice within the landform, radar-wave velocities derived from rock glaciers
280 (Table 2) are likely to serve as a useful proxy for subsurface composition. For example,
281 Monnier & Kinnard (2013) regarded velocities of $0.15\text{--}0.17 \text{ m ns}^{-1}$ within surficial
282 deposits of rock glaciers as evidence of significant quantities of air (high porosity), and
283 calculated that a velocity of 0.16 m ns^{-1} was equivalent to 22% air content. High
284 porosity may explain high velocities near the surface of the lateral complex (Ziii) given
285 the surface sedimentology of boulder-gravel; however, similar velocities are also
286 identified at depth (a time window in excess of 100 ns) within the landform. Buried ice
287 at the margins of high-Arctic glaciers also results in velocities of $0.15\text{--}0.17 \text{ m ns}^{-1}$
288 (Brandt et al. 2007; Midgley et al. 2013). However, the ice within the lateral zone (Ziii)
289 may have a complex origin, and contain both glacier ice and moraine distal snowbank
290 ice (Østrem 1964). Surveys indicate contrasting velocities to that expected in snow

291 (e.g. Table 2). As such, if snow was included into the structure of the landform, it is
292 likely to be of considerable age (potential age ranging from centuries to millennia; e.g.
293 Karlen 1973), resulting in recrystallization, compression and mixing with debris, thus
294 accounting for lower than expected radar-wave propagation velocities for snow as
295 specified in Table 2. An ice-rich substrate in lateral zones would also be consistent
296 with existing interpretations of the adjacent proglacial zone of Storglaciären, where
297 there is disparity in size between the subdued boulder-rich frontal moraine, and larger
298 lateral landforms (Østrem 1964; Karlen 1973; Ackert 1984; Etienne et al. 2003).
299 Interestingly, at Storglaciären, the true-right lateral moraine is noted to have
300 undergone postdepositional modification and slope movement (Karlen 1973; Etienne
301 et al. 2003), which is indicative of an ice-rich substrate, with ice facilitating the transition
302 from moraine to rock glacier.

303 *Internal structure and sedimentology*

304 *Outer-frontal (Zi).* – Profile 1 provides a clear example of sedimentary units deposited
305 on the ice-proximal slope of an existing moraine ridge. Here, the main moraine ridge
306 contained diamicton as demonstrated by radar propagation velocity surveys and direct
307 observation. Subsequent recession of the glacier margin is suggested to have formed
308 a terrace of massive mud within a low energy depositional environment (e.g. an ice-
309 marginal lake). This sedimentary unit was documented in the field, and also appears
310 as a distinct structural unit in profile 1 ('mud'; see Figs 3, 4). The moraine hummock
311 on the distal slope exhibited subhorizontal reflectors, which were found to relate to
312 facies of stratified gravel and sand during ground truth surveys. This unit is interpreted
313 as an ice-contact fan resulting from both gravitational flows and glacialfluvial deposition;
314 however, the relative chronology in relation to other sections of the moraine is unclear
315 (Fig. 4) without further excavation. Ice-proximal deposition appears to be spatially
316 limited across the ridge. The morphological and structural relationships between these
317 sedimentary units suggest that at profile 2 the glacier partially overrode an existing
318 ridge, resulting in two stacked units of diamicton of different ages with a surface
319 contact visible both in-the-field and within the reflection profile.

320 *Inner-frontal (Zii).* – High concentrations of silt – such as are present in many
321 diamictons – are associated with poor signal penetration (e.g. Overgaard & Jakobsen
322 2001). Given the presence of diamicton with the moraines, the strong levels of signal

323 attenuation at depth within the inner-frontal zone (Zii) is highly likely to indicate high
324 silt content within the matrix of the diamicton; a finding consistent with field surveys.
325 The geometry of the radar surfaces (down-glacier dipping) documented here are not
326 consistent with the conceptual model produced by Karlen (1973) who suggested that
327 structurally, moraines largely consist of imbricately arranged units of poorly sorted
328 glacial sediment ('drift sheets'). The origin of the down-glacier dipping structures are
329 uncertain, but assuming that the frontal moraine is ice free (e.g. Østrem 1964; the
330 CMP/WARR data presented here and the high levels of attenuation seen in the
331 reflection survey), the surfaces may relate to bounding layers between stacked units
332 of diamicton. This interpretation would require multiple periods of moraine
333 development and partial overriding of existing moraine obstacles, rather than the
334 proximal enlargement model envisaged by Karlen (1973). Evidence such as the higher
335 levels of clast subangularity in this zone (indicative of subglacial processes), the large
336 size of the frontal moraine, the overprinting of flutes and evidence of overriding of the
337 frontal moraine in 1910, highlight that this landform has a complex origin resulting from
338 multiple periods of development.

339 *Lateral complex (Ziii).* – For Ziii, the hyperbolic radar facies seen in this zone are
340 interpreted as evidence of a predominantly coarse and massive structural
341 configuration, which is consistent with coarse deposits of boulder-gravel found on the
342 moraine surface. Superimposed ridges (e.g. as seen in profile 5) and similar dipping
343 structures to those documented on the frontal-ridge are interpreted as evidence of
344 overriding and distal deposition of material by the glacier on the southern-lateral
345 complex in a similar manner to that envisaged in Zii. Small moraine ridges such as the
346 arcuate ridge visible in profile 5 could have developed in response to the dumping,
347 pushing or squeezing of material at the ice margin (e.g. Price 1970; Birnie 1977;
348 Boulton & Eyles 1979; Bennett 2001; Krüger et al. 2010), or the freeze-on of sediment
349 related to annual oscillations of the ice front (Krüger 1995). Pushing as a moraine
350 forming mechanism is unlikely here as: (i) dominant ice-proximal sediments are
351 dissimilar to those contained within the ridge; (ii) coarse boulder facies have high shear
352 strengths and thus are not particularly conducive to push moraine formation (Cook et
353 al. 2013); and (iii) the ridge contains diamicton with granular lenses, which are linear
354 in form and lack displacement structures associated with ice-marginal stress.

355 Here, subhorizontal and rounded reflectors such as those seen in profiles 6 and 7 are

356 likely to indicate the interface between the surficial deposits of diamicton and boulder-
357 gravel, and an ice-rich substrate at depth. Moorman et al. (2003), for example, found
358 that strong continuous reflectors in GPR surveys undertaken in permafrost terrain
359 were related to the interface between frozen and unfrozen ground conditions. An
360 interpretation of ice-rich permafrost is also consistent with the field observations of
361 Østrem (1964), who excavated the southern-lateral complex, and found ice at depths
362 of 2.2, 2.5 and 2.8 m. Here, for example, the estimated depth to the reflector, thus
363 thickness of the upper surface layer in question, ranges between ~2.25 and ~4.5 m in
364 profile 7.

365 **Discussion**

366 *Development and significance of the Isfallsglaciären moraines*

367 Conceptually, the moraine system at Isfallsglaciären is clearly distinguishable from
368 alpine temperate glacial landsystems, where distinct asymmetrical ice-contact ramps
369 are produced as a result of the flowage of debris from supraglacial positions (Humlum
370 1978; Boulton & Eyles 1979; Röthlisberger & Schneebeli 1979; Small 1983; Lukas &
371 Sass 2011; Lukas et al. 2012). The morphological characteristics of the moraines
372 share some similarity with multi-crested 'controlled' ice-cored moraine complexes
373 documented to occur in some high-Arctic and Icelandic glacial landsystems (Evans
374 2009, 2010; Ewertowski et al. 2012); however, when compared to the geophysical
375 data sets presented in Midgley et al. (2013) there are distinct differences. Midgley et
376 al. (2013) documented very coherent up-glacier dipping reflectors within ice-cored
377 moraine in the Norwegian high-Arctic, which were interpreted as debris-bearing
378 features contained within buried glacier ice; a stark difference to the hyperbolic
379 structures found here, despite the presence of ice within the lateral complex (Ziii). This
380 discrepancy in moraine structure may lend support for a unique mode of ice-
381 incorporation operating at the margins of polythermal glaciers in northern Sweden (e.g.
382 Østrem 1963, 1964).

383 The clast-form data set shows a marked compositional decrease in clast angularity
384 from lateral to frontal zones of the moraine system. Clast-form gradients have been
385 recorded at a number of sites in Scandinavia and Iceland where roundness has been
386 found to decrease with distance from the former glacier terminus (Matthews & Petch
387 1982; Benn & Ballantyne 1994; Spedding & Evans 2002). The clast composition of

388 ice-marginal moraines can relate to the relative importance of passive and active
389 debris transport pathways (e.g. Matthews & Petch 1982; Evans 2010), and the pushing
390 of pre-existing valley side paraglacial debris (e.g. Matthews & Petch 1982). In other
391 areas, the recycling of pre-existing debris by cycles of glacier activity may result in an
392 increase in clast-form 'maturity' (e.g. Burki 2009). In ground-level photography taken
393 by Enqvist in 1910 the glacier surface appears to be relatively free of supraglacial
394 debris leading to well-exposed subglacial sediments within the forefield. Debris can,
395 however, be seen emerging from the ice front, indicating the relative importance of
396 subglacial debris pathways in the frontal zone of the former terminus. The higher
397 proportion of subangular clasts in frontal zones may also demonstrate the importance
398 of processes such as: (i) the accretion of subglacial till onto existing moraine; (ii) the
399 thickening of debris-rich basal ice at the terminus in response to the reverse moraine
400 slope and the cold-based conditions (e.g. Pomeroy 2013); or (iii) the recycling of
401 existing sediment within the glacier forefield (e.g. Burki 2009). Similarities between
402 clast-roundness in profile 3 and profile 4 (e.g. % RA = 46–54), both of which cross-cut
403 more frontal sections of the moraine complex, and control samples from the fluted
404 glacier forefield (% RA = 38, 42 and 44), are likely to reflect the importance of one or
405 more of the above processes.

406 Whilst Karlen (1973) disregarded the ground-level photography taken by Enquist,
407 arguing that proximal enlargement was an important mechanism of moraine
408 development, the structural characteristics (down-glacier dipping reflectors) lend
409 support to the hypothesis of overtopping and distal deposition of debris (profile 2 in Zi
410 and profile 3 in Zii; see Fig. 4). Assuming that the ice margin remains stable over
411 multiple years, mixtures of debris and snow present on the ice-distal face of the
412 moraine will be incorporated into the structure of the landform (e.g. Østrem 1964).
413 Given the limited supraglacial debris visible in the 1910 ground-level photography, the
414 ice margin would need to remain stationary over a considerable period of time to
415 facilitate moraine construction (Boulton & Eyles 1979; Benn et al. 2003). One issue is
416 that debris run out over distal snowbanks is only observed on frontal sections of the
417 moraine in the 1910 ground-level photography (locations approximately delimited in
418 Fig. 4). However, based on interpretation of radar velocity estimates, ice is principally
419 located in the lateral zone (Ziii) of the assessed moraine. The spatial distribution of
420 buried ice inferred from the geophysical surveys presented, however, accord with

421 existing studies in Scandinavia (e.g. Østrem 1964), and also observations in the high-
422 Arctic (e.g. Midgley et al. 2013; Tonkin et al. 2016) where high quantities of buried ice
423 in moraine systems appear to be principally located in lateral ice-marginal areas.

424 An issue requiring further comment is the topographic influence of a pre-existing
425 moraine on glacier geometry (e.g. Spedding & Evans 2002; Barr & Lovell 2014). For
426 the neighbouring Storglaciären, initial moraine formation c. 2.5 ka BP is suggested
427 (Karlen 1973; Ackert 1984; Etienne et al. 2003). On the assumption that the adjacent
428 Isfallsglaciären moraines formed simultaneously, the landforms are highly likely to
429 have exerted a topographic influence on later glacier advance stages. A range of
430 recent Holocene Neoglacial advances between 2.7–2.0, 1.9–1.6, 1.2–1.0 and 0.7–
431 0.2 ka BP were suggested for Scandinavian glaciers by Karlen & Kuylenstierna (1996)
432 with valley glaciers attaining their largest Neoglacial extent during the 17th and 18th
433 centuries (e.g. Karlen 1988; Nesje 2009). Ice-marginal positions demarcated by the
434 previously discussed historical ground-level photography (e.g. photographs taken by
435 Enqvist in 1910; see Fig. 4) and by measurements from 1915 provided by Hamberg
436 et al. (1930) highlight sustained overriding of the inner moraine ridge over a 5-year
437 period between 1910 and 1915 (see Schytt 1959 for a review of historical glacier
438 records). The historical imagery, therefore, demonstrates that overriding is important
439 for the development of the inner-ridge, which, if considered alongside the bounding
440 surfaces identified in radar profile 3, may have occurred at several points in time,
441 resulting in a composite ridge overprinted with flutes (profile 3 in Fig. 4). A discrepancy
442 between moraine size and debris production rate has been suggested to indicate
443 landform development over a time scale in excess of the Little Ice Age at other sites
444 in Scandinavia (Matthews & Petch 1982). Given that the moraines at Isfallsglaciären
445 are likely to also have been developed over long time scales, the push-deformation
446 model as envisaged for a number of high-alpine moraine systems in southern Norway
447 (e.g. Matthews & Shakesby 1984; Shakesby et al. 1987, 2004; Matthews et al. 2014)
448 may also be relevant to Isfallsglaciären, although it is at odds with a model of
449 overriding, which is clearly an important geomorphological process for certain sections
450 (e.g. Zi and Zii) of the Isfallsglaciären moraine system. In summary, the evidence
451 presented in this research highlights that the moraines are likely to be polygenetic in
452 origin, as indicated by observed differences in the internal character and
453 sedimentology across the moraine complex, and time transgressive in age. The

454 resulting geomorphology is a product of the repeated reoccupation of the moraine
455 system by glacier ice, and thus has resulted in what can be described as a 'palimpsest'
456 landsystem (e.g. Pomeroy 2013). The morphological and subsurface characteristics
457 of the outer-frontal moraine (Zi) especially illustrate the composite character of the
458 surveyed moraines.

459 **Reconciling existing geochronologies and structural data**

460 The geochronology of the moraines is currently poorly constrained. The reliability of
461 lichenometric dates from the Isfallsglaciären forefield (e.g. Karlen 1973) are potentially
462 unclear as: (i) the moraine system has been both partially and fully overridden,
463 resulting in the reworking of surface materials; and (ii) the moraine appears to have
464 been subject to extensive snow cover, which at other sites has been linked to reduced
465 confidence in the reliability of lichenometric ages (e.g. Benedict 1993; Osborn et al.
466 2015). Hormes et al. (2004) presented radiocarbon dates from a small valley glacier
467 ~6 km north of Isfallsglaciären. Unlike many moraine systems in the Kebnekaise
468 region, palaeosols were identified within the stratigraphy of these landforms. From the
469 analysis of organic material, Hormes et al. (2004) advocated four periods of soil
470 formation at Nipalsglaciären: 7.8–7.58, 6.3–4.08, 2.45–2.0 and 1.17–0.74 cal. ka BP.
471 Broadly similar responses of Isfallsglaciären to climatic variability during these periods
472 are likely, although it is acknowledged that the two glaciers may have responded
473 differently to environmental change due to site-specific aspect, hypsometry and topo-
474 climate. In the absence of robust dating controls at Isfallsglaciären, and issues with
475 existing lichenometric dates due to the processes of partial glacier self-censoring (e.g.
476 Gibbons et al. 1984; Kirkbride & Winkler 2012), over-extrapolation and snow cover
477 (Osborn et al. 2015), moraine chronologies remain uncertain. Further work could apply
478 additional dating controls; however, it is argued that issues related to the recycling of
479 glacial debris (e.g. Burki 2009) resulting from the overriding of pre-existing
480 materials and potential glacier-permafrost interactions (e.g. Etzelümller & Hagen
481 2005; Matthews et al. 2014) are likely to result in problematic or inconclusive data sets.
482 On this type of landform, traditional geochronological techniques are unsuitable, as
483 the surface appears to post-date the landform (e.g. as indicated by the recent
484 overprinting by flutes). Based on interpretation of the structural data reported here,
485 morphology alone is a poor indicator of glacial history due to the palimpsest nature of
486 the landforms (e.g. Fig. 4), which, despite a probable formation during the mid-late

487 Holocene, have survived periods of glacier re-advance, indicating ineffective self-
488 censoring. As such, great care needs to be employed when interpreting
489 geochronological data obtained from similar landforms. Additional work to document
490 the structural characteristics of a wider range of Scandinavian moraines is a
491 worthwhile endeavour, which may further advance understanding of the glaciological
492 significance of the moraines and facilitate understanding of relict landform
493 assemblages in the geomorphological record.

494 **Conclusions**

495 Radar propagation velocity surveys reported here highlight that the frontal zone of the
496 moraine system at Isfallsglaciären is debris-rich, whereas lateral zones are ice-rich.
497 The lateral zones of the moraines are, however, structurally divergent from ice-cored
498 moraine counterparts in the high-Arctic, revealing hyperbolic and chaotic radar facies.
499 GPR reflection profiles appear to demarcate the spatial extent and depth at which ice
500 within the southern-lateral complex (Ziii) is buried. Radar-depth conversions are in
501 broad agreement with the reported findings of Østrem (1964), indicating ice at depths
502 of ~2.25–4.50 m along profile 7. Given that previously destructive methods were used
503 to investigate moraine structure, GPR is shown to be a valuable tool for documenting
504 the structure of ice-marginal landforms. The frontal landforms are complex in form,
505 and whilst in places (e.g. parts of Zi) the ridges may represent former ice-marginal
506 positions resulting from Holocene glacier re-advances, in others, overriding has
507 reworked surface materials (e.g. Zii). It is unclear whether the transmission of stress
508 onto pre-existing ridges has influenced the morphology of the investigated moraine
509 system. The application of traditional geochronological methods are unlikely to provide
510 a useful measure of moraine age due to the palimpsest nature of the moraine system,
511 which has most likely developed as a result of repeated occupation of the glacier
512 forefield over the course of the Holocene. It is hoped that the data set provided here
513 will not only facilitate greater understanding of the geochronology, and likely mode of
514 formation of ice-marginal moraine at polythermal glaciers, but also aid interpretations
515 of relict landform assemblages in glaciated valley landsystems.

516 *Acknowledgements.* – T. N. Tonkin undertook this research whilst funded by a
517 Nottingham Trent University VC Bursary. This research received funding from the
518 European Union Seventh Framework Programme (FP7/2007-2013) under grant

519 agreement no 262693 (INTERACT). Prof. Gunhild Rosqvist and the staff at Tarfala
520 Research Station are thanked for providing logistical support. The reviewers and editor
521 are thanked for helpful comments on the work. The authors also thank Esther Kettel
522 for proof-reading an early draft of this manuscript.

523 **References**

524 Ackert, R. P. 1984: Ice-cored lateral moraines in Tarfala Valley, Swedish Lapland.
525 *Geografiska Annaler* 66, 79–88.

526 Barr, I. D. & Lovell, H. 2014: A review of topographic controls on moraine distribution.
527 *Geomorphology* 226, 44-64.

528 Barsch, D. 1971: Rock glaciers and ice-cored moraines. *Geografiska Annaler* 53, 203–
529 206.

530 Benedict, J. B. 1993: A 2000-year lichen-snowkill chronology for the Colorado Front
531 Range, USA. *The Holocene* 3, 27–33.

532 Benn, D. I. & Ballantyne, C. K. 1994: Reconstructing the transport history of glacial
533 sediments: a new approach based on the co-variance of clast form indices.
534 *Sedimentary Geology* 91, 215-227.

535 Benn, D. I. 2004: Clast morphology. In Evans, D. J. A. & Benn, D. I. (eds.): A Practical
536 Guide to the Study of Glacial Sediments, 77–92. Arnold, London.

537 Benn, D. I., Kirkbride, M. P., Owen, L. A. & Brazier, V. 2003: Glaciated valley
538 landsystems. In Evans, D.J.A. (ed.) *Glacial Landsystems*. Arnold, London, 372-406.

539 Bennett, M. R. 2001: The morphology, structural evolution and significance of push
540 moraines. *Earth-Science Reviews* 53, 197–236.

541 Berthling, I. 2011: Beyond Confusion: Rock glacier as cryo-conditioned landforms.
542 *Geomorphology* 131, 98–106.

543 Birnie, R. V. 1977: A snow-bank push mechanism for the formation of some "annual"
544 moraine ridges. *Journal of Glaciology* 18, 77–85.

545 Boulton, G. S. & Eyles, N. 1979: Sedimentation by valley glaciers: a model and genetic
546 classification. In Schlüchter, C. (ed.): *Moraines and Varves: Origin, Genesis,*
547 *Classification*, 11–23. Balkema, Rotterdam.

- 548 Brandt, O., Langley, K., Kohler, J. & Hamran, S-K. 2007: Detection of buried ice and
549 sediment layers in permafrost using multi-frequency Ground Penetrating Radar: A
550 case examination on Svalbard. *Remote Sensing of Environment* 111, 212–227.
- 551 Brugger, K. A. & Pankratz, L. 2015: Changes in the geometry and volume of Rabots
552 glaciär, Sweden, 2003–2011: Recent accelerated volume loss linked to more negative
553 summer balances. *Geografiska Annaler* 97, 265–278.
- 554 Burki, V. 2009: Glacial remobilization cycles as revealed by lateral moraine sediment,
555 Bødalsbreen glacier foreland, western Norway. *The Holocene* 19, 415–426.
- 556 Burki, V., Larsen, E., Fredin, O. & Margreth A. 2009: The formation of sawtooth
557 moraine ridges in Bødalen, western Norway. *Geomorphology* 105, 182–192.
- 558 Carrivick, J. L., Smith, M. W. & Carrivick, D. M. 2015: Terrestrial laser scanning to
559 deliver high-resolution topography of the upper Tarfala valley, arctic Sweden. *GFF* 137,
560 383–396.
- 561 Cook, S. J., Porter, P. R. & Bendall, C. A. 2013: Geomorphological consequences of a
562 glacier advance across a paraglacial rock avalanche deposit. *Geomorphology* 189,
563 109–120.
- 564 Degenhardt, Jr, J. J. & Giardino, J. R. 2003. Subsurface investigation of a rock glacier
565 using ground-penetrating radar: Implications for locating stored water on Mars. *Journal*
566 *of Geophysical Research: Planets* 108 (E4), 8036.
- 567 Degenhardt, Jr, J. J. 2009: Development of tongue-shaped and multilobate rock
568 glaciers in alpine environments – Interpretations from ground penetrating radar
569 surveys. *Geomorphology* 109, 94–107.
- 570 Eklund, A. & Hart, J.K., 1996: Glaciotectonic deformation within a flute from the
571 Isfallsglaciären, Sweden. *Journal of Quaternary Science* 11 (4), 299-310.
- 572 Etienne, J. L., Glasser, N. F. & Hambrey, M. J. 2003: Proglacial sediment–landform
573 associations of a polythermal glacier: Storglaciären, northern Sweden. *Geografiska*
574 *Annaler* 85, 149–164.
- 575 Etzelmüller, B. & Hagen, J. O. 2005: Glacier permafrost interaction in arctic and alpine
576 environments – examples from southern Norway and Svalbard. In Harris, C. & Murton,

- 577 J. (eds.): Cryospheric systems – Glaciers and Permafrost. British Geological Society,
578 Special Publications, 242, pp 11–27.
- 579 Evans, D. J. A. 2009: Controlled moraines: origins, characteristics and
580 palaeoglaciological implications. *Quaternary Science Reviews* 28, 183–208.
- 581 Evans, D. J. A. 2010: Controlled moraine development and debris transport pathways
582 in polythermal plateau icefields: examples from Tungnafellsjökull, Iceland. *Earth*
583 *Surface Processes and Landforms* 35 (12), 1430-1444.
- 584 Ewertowski, M., Kasprzak, L., Szuman, I. & Tomczyk, A.M. 2012: Controlled, ice-cored
585 moraines: sediments and geomorphology. An example from Ragnarbreen, Svalbard.
586 *Zeitschrift für Geomorphologie* 56, 53–74.
- 587 Gibbons, A. B., Megeath, J. D. & Pierce, K. L. 1984: Probability of moraine survival in
588 a succession of glacial advances. *Geology* 12, 327–330.
- 589 Goldthwait, R. P. 1951. Development of end moraines in east-central Baffin Island.
590 *The Journal of Geology* 59, 567–577.
- 591 Gusmeroli, A., Jansson, P., Pettersson, R. & Murray, T. 2012: Twenty years of cold
592 surface layer thinning at Storglaciären, sub-Arctic Sweden, 1989-2009. *Journal of*
593 *Glaciology* 58, 3–10.
- 594 Hamberg, A., Rabot, C. & Mercanton, P.L. 1930: *Commission UGGI des glaciers:*
595 *Rapport pour 1914 – 1928.* Venezia 1930. 1–53.
- 596 Hambrey, M. J. 1994: *Glacial Environments.* 296 pp. University College Press,
597 London.
- 598 Heyman, J. & Hättstrand C. 2006: Morphology, distribution and formation of relict
599 marginal moraines in the Swedish mountains. *Geografiska Annaler* 88, 253–265.
- 600 Holmlund, P. & Jansson P. 1999: The Tarfala mass balance programme. *Geografiska*
601 *Annaler* 81, 621–631.
- 602 Holmlund, P., Karlén, W. & Grudd, H. 1996: Fifty years of mass balance and glacier
603 front observations at the Tarfala Research Station. *Geografiska Annaler* 78, 105–114.

604 Hormes, A., Karlén, W. & Possnert G. 2004: Radiocarbon dating of palaeosol
605 components in moraines in Lapland, northern Sweden. *Quaternary Science Reviews*
606 23, 2031–2043.

607 Humlum, O. 1978: Genesis of layered lateral moraines: Implications for
608 palaeoclimatology, and lichenometry. *Geografisk Tidsskrift* 77, 65–72.

609 Karlén, W. & Kuylenstierna J. 1996: On solar forcing of Holocene climate: evidence
610 from Scandinavia. *The Holocene* 6, 359–365.

611 Karlén, W. 1973: Holocene glacier and climatic variations, Kebnekaise mountains,
612 Swedish Lapland. *Geografiska Annaler* 55, 29–63.

613 Karlén, W. 1988: Scandinavian glacial and climatic fluctuations during the Holocene,
614 *Quaternary Science Reviews* 7, 199–209.

615 Kirkbride, M. P. & Winkler, S. 2012: Correlation of Late Quaternary moraines: impact
616 of climate variability, glacier response, and chronological resolution. *Quaternary*
617 *Science Reviews* 46, 1–29.

618 Kneisel, C. 2010: Frozen ground conditions in a subarctic mountain environment,
619 Northern Sweden. *Geomorphology* 118 (1), 80–92.

620 Krüger, J. & Kjær, K.H. 2000: De-icing progression of ice-cored moraines in a humid,
621 subpolar climate, Kötluökull, Iceland. *The Holocene* 10, 737–747.

622 Krüger, J. 1995: Origin, chronology and climatological significance of annual-moraine
623 ridges at Mýrdalsjökull, Iceland. *The Holocene* 5, 420–427.

624 Krüger, J., Schomacker, A. & Benediktsson, Í. Ö. 2010: Ice-marginal environments:
625 geomorphic and structural genesis of marginal moraines at Mýrdalsjökull. In
626 Schomacker, A., Krüger, J. & Kjær, K. H. (eds.): *The Mýrdalsjökull Ice Cap, Iceland.*
627 *Glacial processes, sediments and landforms on an active volcano. Developments in*
628 *Quaternary Science* 13, 79–104.

629 Lindhorst, S. & Schutter, I. 2014: Polar gravel beach-ridge systems: Sedimentary
630 architecture, genesis, and implications for climate reconstructions (South Shetland
631 Islands/Western Antarctic Peninsula). *Geomorphology* 221, 187–203.

- 632 Lukas, S. & Sass, O. 2011: The formation of Alpine lateral moraines inferred from
633 sedimentology and radar reflection patterns: a case study from Gornergletscher,
634 Switzerland. In Martini, I. P., French, H. M. & Pérez Alberti, A. (eds.): *Ice-Marginal and*
635 *Periglacial Processes and Sediments*, Geological Society, London, *Special*
636 *Publications 354*, 77–92.
- 637 Lukas, S., Graf, A., Coray, S. & Schlüchter C. 2012: Genesis, stability and preservation
638 potential of large lateral moraines of Alpine valley glaciers – towards a unifying theory
639 based on Findelengletscher, Switzerland. *Quaternary Science Reviews 38*, 27–48.
- 640 Matthews, J. A. & Petch, J. R. 1982: Within valley asymmetry and related problems of
641 Neoglacial lateral moraine development at certain Jotunheimen glaciers, southern
642 Norway. *Boreas 11*, 225–247.
- 643 Matthews, J. A., Winkler, S. & Wilson P. 2014: Age and origin of ice-cored moraines in
644 Jotunheimen and Breheimen, southern Norway: insights from Schmidt-hammer
645 exposure-age dating. *Geografiska Annaler 96*, 531–548.
- 646 Matthews, J.A. & Shakesby, R.A. 1984: The status of the ‘Little Ice Age’ in southern
647 Norway: relative-age dating of Neoglacial moraines with Schmidt hammer and
648 lichenometry. *Boreas 13*, 333–346.
- 649 Midgley, N. G., Cook, S. J., Graham, D. J. & Tonkin, T. N. 2013: Origin, evolution and
650 dynamic context of a Neoglacial lateral–frontal moraine at Austre Lovénbreen,
651 Svalbard. *Geomorphology 198*, 96–106.
- 652 Monnier, S. & Kinnard, C. 2013. Internal structure and composition of a rock glacier in
653 the Andes (upper Choapa valley, Chile) using borehole information and ground-
654 penetrating radar. *Annals of Glaciology 54*, 61–72.
- 655 Moorman, B. J., Robinson, S. D. & Burgess, M. M. 2003: Imaging periglacial conditions
656 with ground-penetrating radar. *Permafrost and Periglacial Processes 14*, 319–329.
- 657 Murrery, T., Stuart, G. W., Miller, P. J., Woodward, J., Smith, A. M., Porter, P.R. &
658 Jiskoot, H. 2000: Glacier surge propagation by thermal evolution at the bed. *Journal*
659 *of Geophysical Research: Solid Earth 105*, 13491–13507.
- 660 Neal, A. 2004: Ground-penetrating radar and its use in sedimentology: principles,
661 problems and progress. *Earth-Science Reviews 66*, 261–330.

- 662 Nesje, A. 2009: Latest Pleistocene and Holocene alpine glacier fluctuations in
663 Scandinavia. *Quaternary Science Reviews* 28, 2119–2136.
- 664 Osborn, G., McCarthy, D., LaBrie, A. & Burke, R. 2015: Lichenometric dating: Science
665 or pseudo-science? *Quaternary Research* 83, 1–12.
- 666 Østrem, G. 1959: Ice melting under a thin layer of moraine, and the existence of ice
667 cores in moraine ridges. *Geografiska Annaler* 41, 228–230.
- 668 Østrem, G. 1963: Comparative crystallographic studies on ice from ice-cored moraine,
669 snow banks and glaciers. *Geografiska Annaler* 45, 210–40.
- 670 Østrem, G. 1964: Ice-cored moraines in Scandinavia. *Geografiska Annaler* 46, 282–
671 337.
- 672 Østrem, G. 1965: Problems of dating ice-cored moraines. *Geografiska Annaler* 47, 1–
673 38.
- 674 Østrem, G. 1971: Rock Glaciers and Ice-Cored Moraines, a Reply to D. Barsch.
675 *Geografiska Annaler* 53, 207–213.
- 676 Overgaard, T. & Jakobsen, P.R. 2001: Mapping of glaciotectonic deformation in an ice
677 marginal environment with ground penetrating radar. *Journal of Applied Geophysics*
678 47, 191–197.
- 679 Pellicer, X. M. & Gibson, P. 2011: Electrical resistivity and Ground Penetrating Radar
680 for the characterisation of the internal architecture of Quaternary sediments in the
681 Midlands of Ireland. *Journal of Applied Geophysics* 75, 638–647.
- 682 Pettersson, R., Jansson, P. & Holmlund, P. 2003: Cold surface layer thinning on
683 Storglaciären, Sweden, observed by repeated ground penetrating radar surveys.
684 *Journal of Geophysical Research: Earth Surface* 108 (F1).
- 685 Pomeroy, J. A. 2013: The sedimentary and geomorphic signature of subglacial
686 processes in the Tarfala Valley, northern Sweden, and the links between subglacial
687 soft-bed deformation, glacier flow dynamics, and landform generation. Ph.D. thesis,
688 Loughborough University, 408 pp.
- 689 Powers, M. C. 1953: A new roundness scale for sedimentary particles. *Journal of*
690 *Sedimentary Research* 23, 117–119.

691 Price, R. J. 1970: Moraines at Fjallsjökull, Iceland. *Arctic and Alpine Research* 2, 27–
692 42.

693 Reynolds, J. M. 2011: *An Introduction to Applied and Environmental Geophysics*. 696
694 pp. John Wiley & Sons, New York.

695 Rippin, D. M., Carrivick, J. & Williams C. 2011: Evidence towards a thermal lag in the
696 response of Kårsaglaciären, northern Sweden, to climate change. *Journal of*
697 *Glaciology* 57, 895–903.

698 Röthlisberger, F. & Schneebeli, W. 1979: Genesis of lateral moraine complexes,
699 demonstrated by fossil soils and trunks: indicators of postglacial climatic fluctuations.
700 In Schlüchter, C. (ed.): *Moraines and Varves*. Balkema, Rotterdam, 387–419.

701 Sass, O. & Krautblatter, M. 2006: Debris flow-dominated and rockfall-dominated talus
702 slopes: Genetic models derived from GPR measurements. *Geomorphology* 86, 176–
703 192.

704 Schomacker, A. & Kjær, K. H. 2008: Quantification of dead-ice melting in ice-cored
705 moraines at the high-Arctic glacier Holmströmbreen, Svalbard. *Boreas* 37, 211–225.

706 Schwamborn, G., Heinzl, J. & Schirrmeyer, L. 2007: Internal characteristics of ice-
707 marginal sediments deduced from georadar profiling and sediment properties
708 (Brøgger Peninsula, Svalbard). *Geomorphology* 95, 74–83.

709 Schytt, V. 1959: The Glaciers of the Kebnekajse-Massif. *Geografiska Annaler* 41, 213–
710 227.

711 Schytt, V. 1962: A tunnel along the bottom of Isfallsglaciären. *Geografiska Annaler* 44,
712 411–412.

713 Schytt, V. 1966: Notes on Glaciological Activities in Kebnekaise, Sweden during 1965.
714 *Geografiska Annaler* 48, 43–50.

715 Shakesby, R. A., Matthews, J. A. & Winkler, S. 2004: Glacier variations in Breheimen,
716 southern Norway: relative-age dating of Holocene moraine complexes at six high-
717 altitude glaciers. *The Holocene* 14, 899–910.

718 Shakesby, R.A., Dawson, A.G. & Matthews, J.A. 1987: Rock glaciers, protalus
719 ramparts and related phenomena, Rondane, Norway: a continuum of large-scale talus
720 derived landforms. *Boreas* 16, 306–317.

721 Small, R. J. 1983: Lateral moraines of Glacier De Tsidjiore Nouve: form, development
722 and implications. *Journal of Glaciology* 29, 250–259.

723 Spedding, N. & Evans, D. J. A. 2002: Sediments and landforms at Kviárjökull,
724 southeast Iceland: a reappraisal of the glaciated valley landsystem. *Sedimentary*
725 *Geology* 149, 21–42.

726 Sugden, D. E., Marchant, D. R., Potter, N., Souchez, R. A., Denton, G. H., Swisher, C.
727 C. & Tison, J. L. 1995: Preservation of Miocene Glacier Ice in East Antarctica, *Nature*
728 376 (6539), 412-414

729 Tonkin, T. N., Midgley, N. G., Cook, S. J. & Graham, D. J. 2016: Ice-cored moraine
730 degradation mapped and quantified using an Unmanned Aerial Vehicle: A case study
731 from a polythermal glacier in Svalbard. *Geomorphology* 258, 1-10.

732 Whalley, W. B. & Martin, H. E. 1992: Rock glaciers: II models and mechanisms.
733 *Progress in Physical Geography* 16, 127–186.

734 Whalley, W. B. 2009: On the interpretation of discrete debris accumulations associated
735 with glaciers with special reference to the British Isles. In: Knight, J. and Harrison, S.
736 (eds), *Periglacial and Paraglacial Processes and Environments*. The Geological
737 Society, London, Special Publications 320, 85–102.

738 Winkler, S. & Matthews, J.A. 2010: Observations on terminal moraine-ridge formation
739 during recent advances of southern Norwegian glaciers. *Geomorphology* 116 (1), 87-
740 106.

741 Zemp, M., Jansson, P., Holmlund, P., Gärtner-Roer, I., Koblet, T., Thee, P. & Haeberli,
742 W. 2010: Reanalysis of multi-temporal aerial images of Storglaciären, Sweden (1959–
743 99) – Part 2: Comparison of glaciological and volumetric mass balances. *The*
744 *Cryosphere* 4, 345–357.

745 **Fig. 1.** The location of Isfallsglaciären in relation to Scandinavia. The locations of the
746 geophysical surveys reported are displayed over a hillshaded model of the moraines
747 produced from data provided by Carrivick et al. (2015).

748

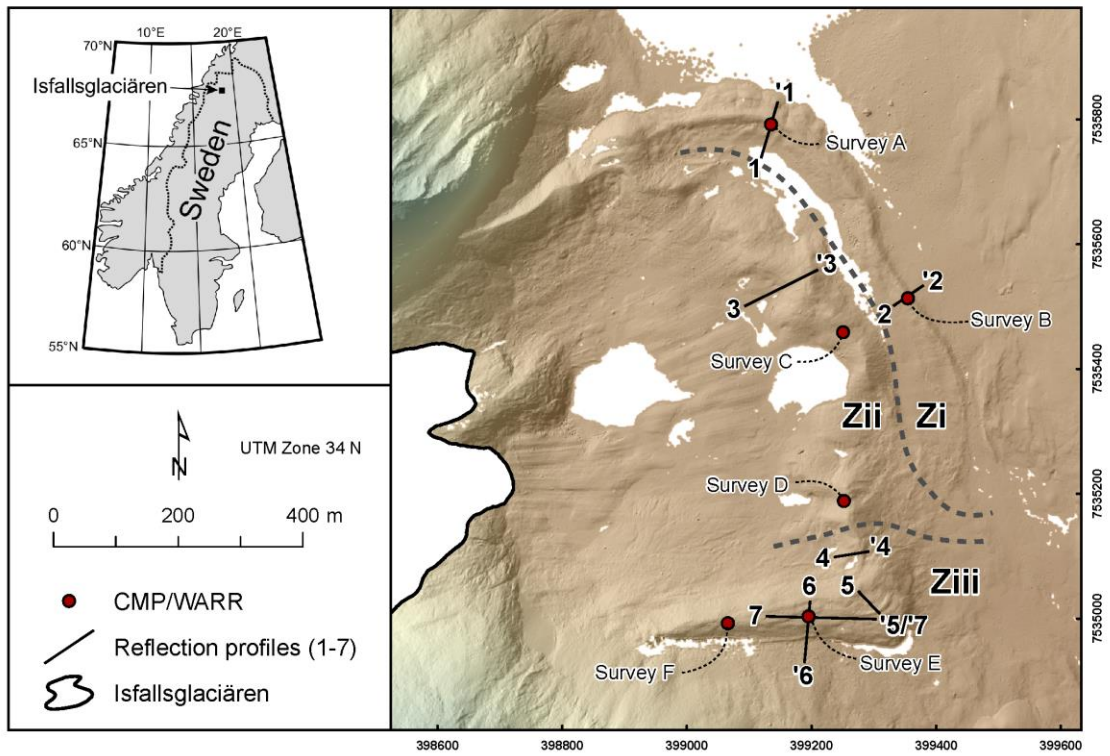
749 **Fig. 2.** Plots showing the radar wave propagation velocity at different locations across
750 the moraine complex. Note how propagation velocity is increased at lateral positions.

751

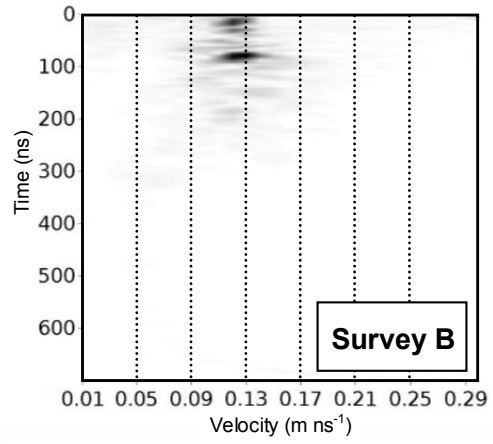
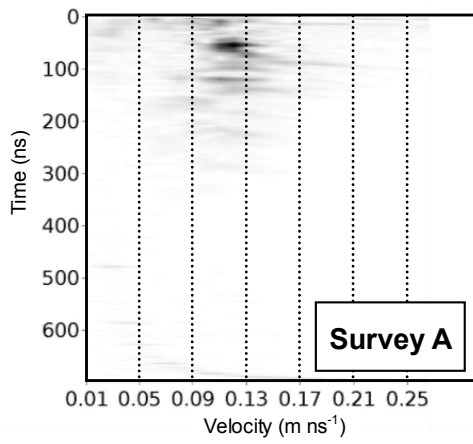
752 **Fig. 3.** Topographically migrated GPR reflection surveys. Profiles 1–6 cross cut the
753 moraine crestline, with the ice-proximal slope to the right. Approximately 25 m along
754 profile 6, the transect cuts across profile 7. Profile 7 runs approximately parallel to the
755 moraine crestline with up-glacier sections of the landform to the right, and crosses
756 profile 6 at ~68 m along the transect. Profile 7 has not been adjusted for topography.

757

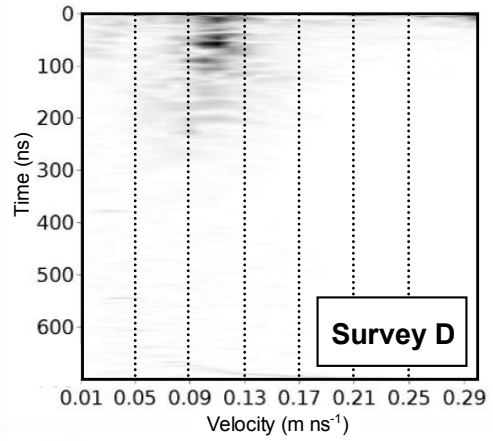
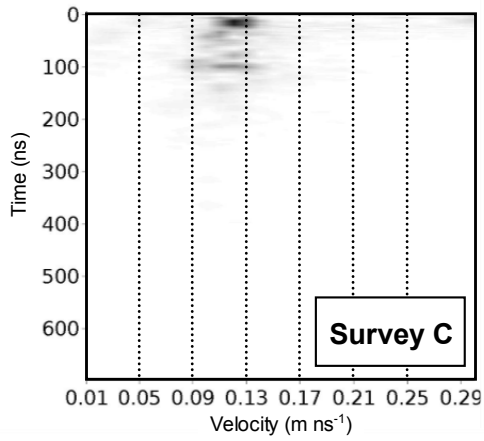
758 **Fig. 4.** An illustration of the former glacier in 1910 and an interpretation of the ice-
759 marginal moraines within the different zones.



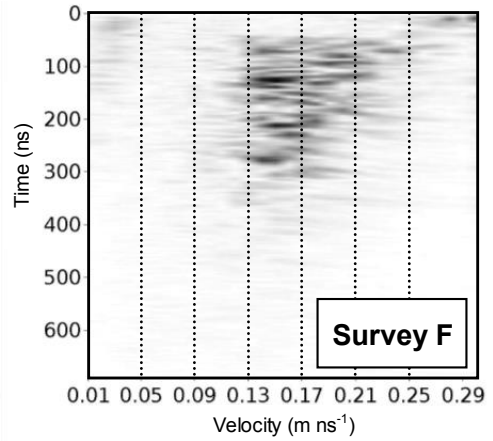
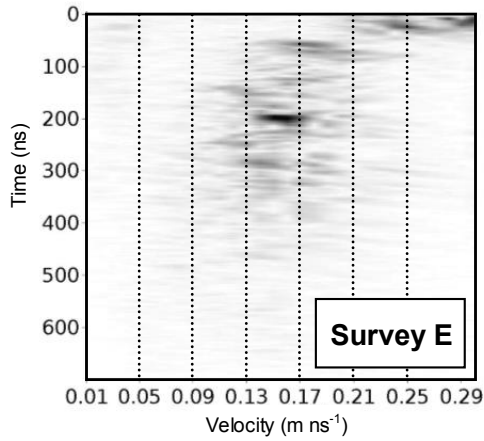
Outer-frontal (Zi):

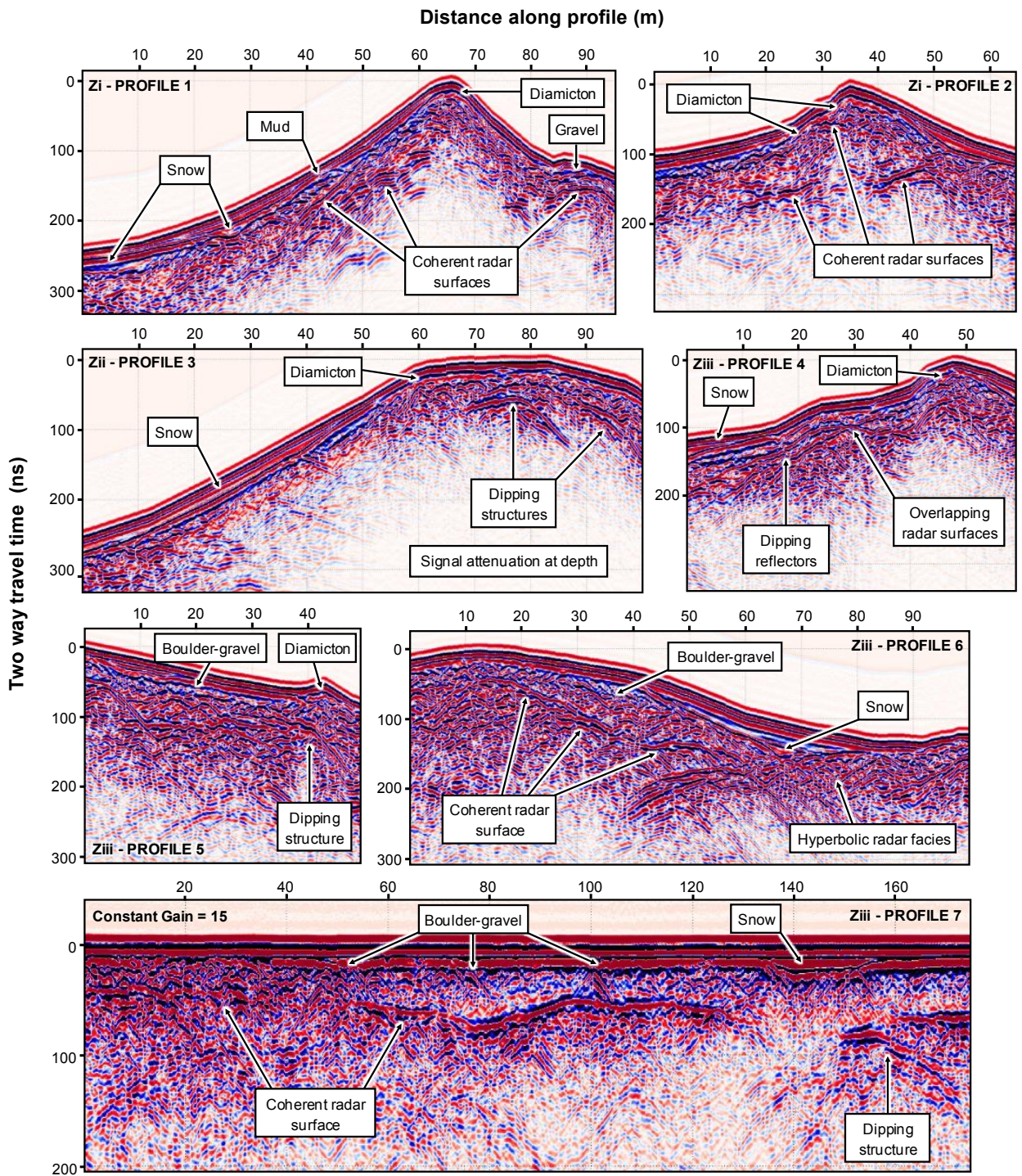


Inner-frontal (Zii):



Lateral complex (Ziii):



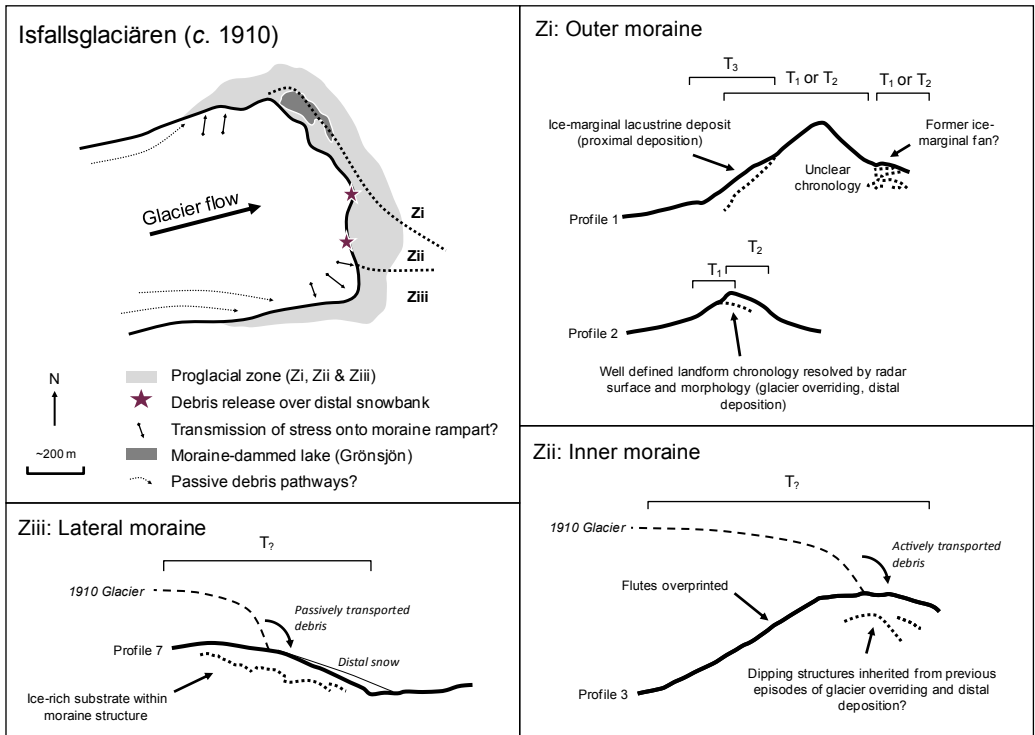


Time/depth conversion: Depth = $v \times \text{TWTT} / 2$

AGC applied to all profiles (unless stated)

100 ns = 5 metres (if $v = 0.10 \text{ m ns}^{-1}$)

7.5 metres (if $v = 0.15 \text{ m ns}^{-1}$)



764 **Table 1.** Summary of interpreted radar facies.

<i>Zone</i>	<i>Profile</i>	<i>Radar-surface geometries</i>	<i>Radar facies</i>	<i>Signal attenuation</i>	<i>Surficial sedimentology</i>	<i>Likely composition</i>
Zi	1	Dipping up glacier; Sub-horizontal to the moraine surface	Chaotic	High	Mud, diamicton, gravel	Debris
	2	Dipping up glacier; Dipping down glacier	Chaotic	High	Diamicton	Debris
Zii	3	Dipping down glacier; Sub-parallel to the moraine surface	Chaotic	High	Diamicton	Debris
Ziii	4	Dipping up glacier; Sub-parallel to the moraine surface	Chaotic	Moderate	Diamicton	Debris-ice mix?
	5	Dipping down glacier; Sub-parallel to the moraine surface	Chaotic; Hyperbolic	Low	Boulder-gravel, diamicton	Debris-ice mix
	6	Dipping down glacier; Sub-parallel to the moraine surface	Chaotic; Hyperbolic	Low	Boulder-gravel, diamicton	Debris-ice mix
	7	Dipping down glacier; Sub-parallel to the moraine surface	Chaotic; Hyperbolic	Low	Boulder-gravel, diamicton	Debris-ice mix

766 **Table 2.** Radar velocities for a range of landforms and features.

Substrate	Velocity ($m\ ns^{-1}$)	Source(s)
Air	0.3	Reynolds (2011)
Snow	0.194–0.252	Reynolds (2011)
Glacial sediment	0.06–0.10	Sass & Krautblatter (2007); Lukas & Sass (2011); Burki <i>et al.</i> (2009)
Diamicton (frozen)	0.115–0.135	Brandt <i>et al.</i> (2007); Schwamborn <i>et al.</i> (2008)
Loose talus	0.11–0.14	Sass & Krautblatter (2007)
Rock glacier	0.12–0.17	Degenhardt Jr. & Giardino (2003); Degenhardt Jr. (2009); Monnier & Kinnard (2013)
Glacier ice	0.167–0.170	Murray <i>et al.</i> (2000)
Buried ice	0.15–0.17	Brandt <i>et al.</i> (2007); Midgley <i>et al.</i> (2013)